Supplementary Information (SI) for RSC Sustainability.
This journal is © The Royal Society of Chemistry 2024

Supporting Information

Sustainable micro-cellulosic additives for high-density fiber cement: Emphasis on rheo-mechanical properties and cost-performance analysis

Sreenath Raghunath [a,b], *Mahfuzul Hoque* [a,b], *Behzad Zakani* [a,b], *Akash Gondaliya* [a,b],

E. Johan Foster [a,b]*

[a] Department of Chemical and Biological Engineering, The University of British Columbia. 2385 East Mall, Vancouver, BC Canada V6T 1Z4.

and

[b] Bioproducts Institute, 2385 East Mall Vancouver, BC Canada V6T 1Z4.

Email Address: johan.foster@ubc.ca

This supporting information contains 14 pages (S1-S14), 7 figures (S1-S7), 13 tables (S1-S13)

Experimental

Materials and Methods

Raw materials physical properties

Table S1. General Composition of ordinary Portland cement [1]

Clinker Phases	Quantity (%)
Tricalcium silicates (C_3S)	30-55
Dicalcium silicates (C_2S)	20-50
Tricalcium aluminate (C_3A)	7-12
Tetracalcium aluminoferrite (C_4AF)	6-11

Table S2. Physio-chemical properties of OPC (procured from Lafarge, Canada) used for this research. [2]

Components	Quantity (%)
Limestone	≤15
Gypsum	2-10
Magnesium Oxide	≤4
Quartz	≤0.2
Physiochemical properties	
Physical state	Solid
Color	Gray, off white or white powder
PH	12 -13 (in water)
Boiling point	> 1000 °C
Specific Gravity	3.15 (water = 1)

Table S3. Physiochemical properties of Avicel® Ph 101 (procured from sigma Aldrich, Canada) used for this research.[3]

Properties	
CAS number	9004-34-6
Appearance	White, powder
Moisture content	3 – 5 %
Loose bulk density	0.26-0.31 gcm^{-1}
BET surface area	1220 m^2/kg
PH	5.5 – 7.0
Degree of polymerization	NMT 350 units

Table S4. Physiochemical properties of Alpha cellulose (sigma Aldrich, Canada) used for this research.

Properties	
CAS number	9004 -34 -6
Source	Plant
Appearance	White / off white (fiber) powder
Bulk density	5.6 – 6.8 cc/g

Table S5. Properties of cellulose nanocrystals (CNC), which was procured from the product development center, University of Maine, USA) for this research.[4]

Properties	
Appearance	White / off white
Density	1.5 g/cm^3
Width	5 -20 nm
Length	150 – 200 nm
Aspect ratio	10 - 30
Sulphur content (in dry CNCs)	0.85 wt.% Sulphur
Solid content	98% dry powder

Table S6. Properties of northern bleached softwood Kraft (NBSK) pulp.[5,6] The bleaching process, ECF stands for Enhanced – Elemental chlorine free. And the beaching sequence, $DE_{OP}DE_PD$ stands for D-Chlorine dioxide reacts with pulp in acidic medium. E – Dissolution of reaction product with oxygen. O-Molecular oxygen reacts with pulp in alkaline medium at high pressure. P – Peroxide reacts with pulp in alkaline medium.

Properties	
Species	Lodgepole pine – Pinus contorta, white spruce – Picea glauca, Sub–alpine fir–Abies lasiocarpa
Bleaching Process	ECF
Bleaching sequence	$DE_{OP}DE_PD$

Table S7. Refined (PFI mill) properties of NBSK fiber used for this research.

Properties	
Revolutions	4500
Coarseness	0.157 mg/m
Freeness	621.3 ml
Curl Index (Length weighted)	0.184
Kink Index	2.11 (1/mm)
Total Kink angle	71.88 Degrees
Kinks /mm	0.94 (1/mm)

Table S8. Physical properties of the commercial polycarboxylate (PCEs) based superplasticizer, that is, poly(acrylamide-co-acrylic acid) partial sodium salt.

Appearance	**White to off white**
Molecular weight (kDa)	M_w: 520
	M_n: 150
Viscosity (cP) @ 25 °C	150-700
Particle size (µm)	150.05

Mechanical characterization

Table S9. The yield stress and modulus of rupture values of fiber cement paste containing varying proportions of NBSK fibers and cellulose nanocrystals (CNC). * Indicates that the value was obtained from the current study.

Sample name	**Modulus of Rupture (MPa)**	**Yield stress (Pa)**	**NBSK content (wt.%)**	**CNC content (wt.%)**
FC_NBSK_10%_CNC_2%	8.2[7]	68*	10	2
FC_NBSK_8%_CNC_4%	8.5[7]	74*	8	4

Microscopic Characterization

(a)

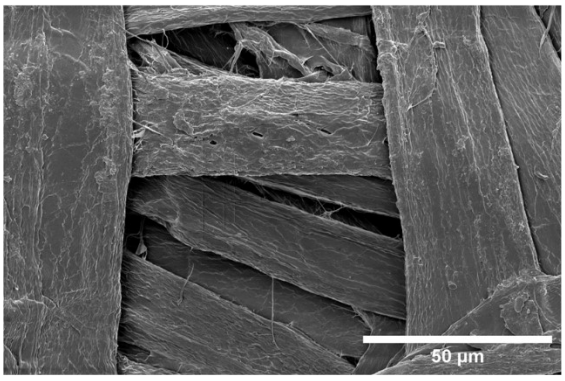

(b)

Refined NBSK fiber properties	**Dimension (µm)**
Fiber length (L)	1386
Fiber width (W)	27.7
Fiber aspect ratio	50

Figure S1. Fiber size and morphology characterization. Physical properties of refined NBSK fiber (wet form). We refined the fiber for 4500 revolutions using the PFI mill and conducted the size characterization using FQA (detailed in the experimental section, main manuscript).

To ascertain the physical properties (length, width, curl, kink, freeness, aspect ratio and coarseness) of the NBSK fibers after refining, we utilized a high-resolution fiber quality analyzer from OpTest Equipment Inc, Canada (Mode: FQA-30). The experimental methodology and principles of FQA were followed as per the guidelines described in detail by Robertson & Olson et al.[23]

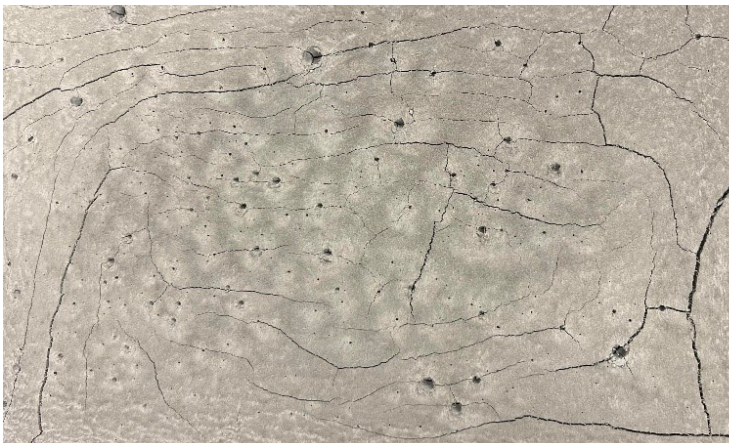

Figure S2. Image of fiber cement sample containing 10 wt.% MCC content and 2 wt.% NBSK fibers. Note that the samples cracked within one day of curing.

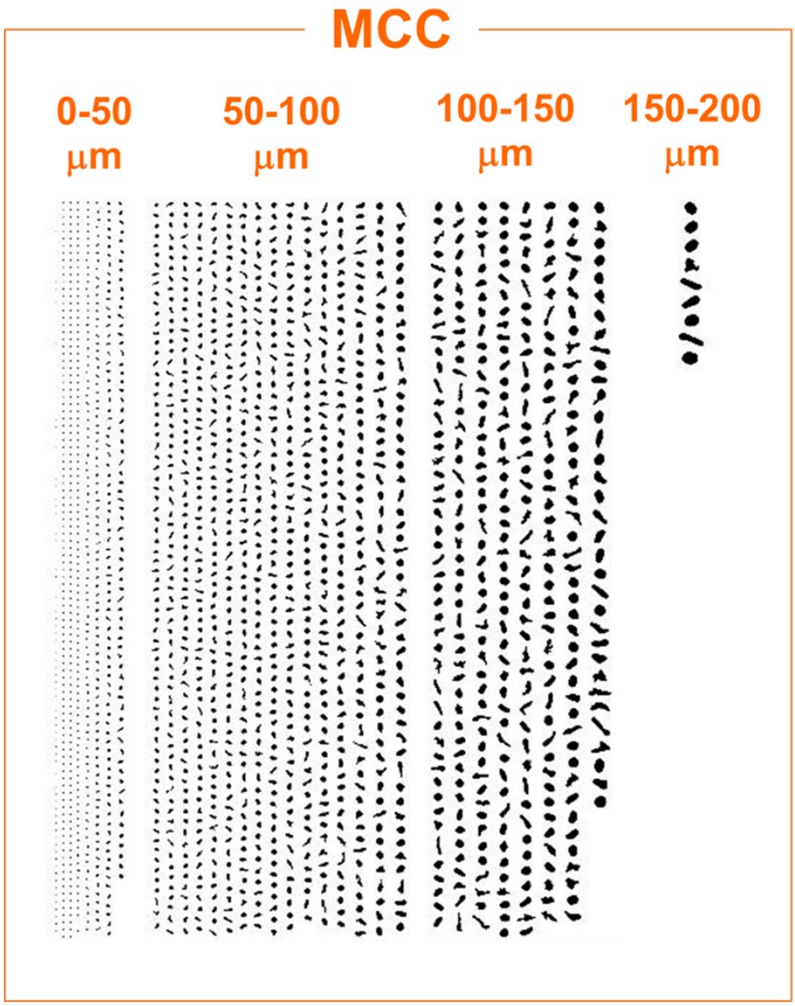

Figure S3. A digital mosaic of individual MCC particle in motion as a function of particle size. Image captured during the dynamic image analysis (DIA) measurement.

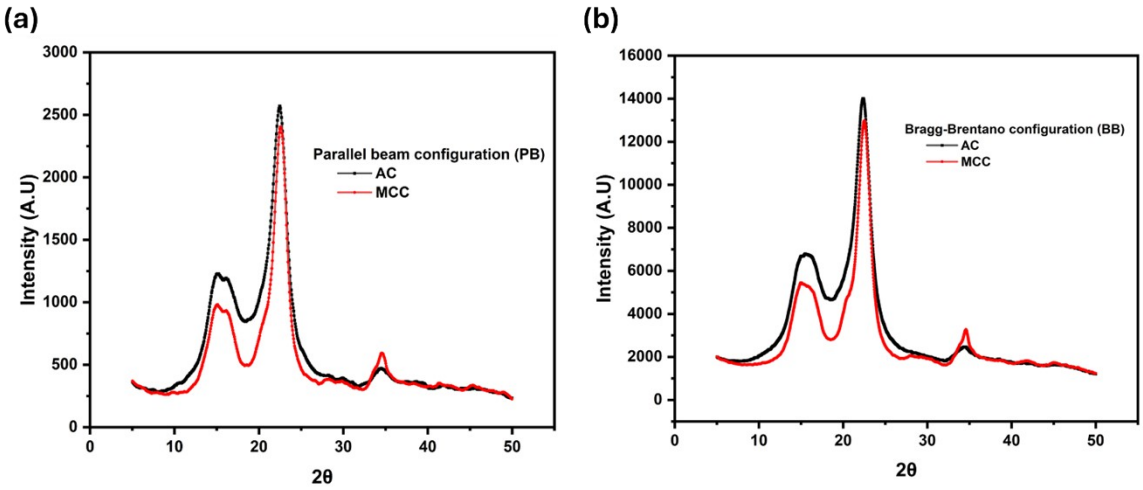

Figure S4. Representative PXRD diffractograms of micro-additives (AC and MCC) employed for this study computed using two different configuration modes (a) Parallel beam (PB) and (b) Bragg-Brentano configurations respectively.

Table S10. Crystallinity index (C*ri*) of AC and MCC, calculated using Segal's method[8].

Additives	**Crystallinity index (*CI*) % (PB configuration)**	**Crystallinity index (C*I*) % (BB configuration)**
Alpha cellulose (AC)	67.4%	67.1 %
Microcrystalline cellulose (MCC)	79.62%	78.57%

The calculated *CI* values were in accordance reported in literatures.[9–12]

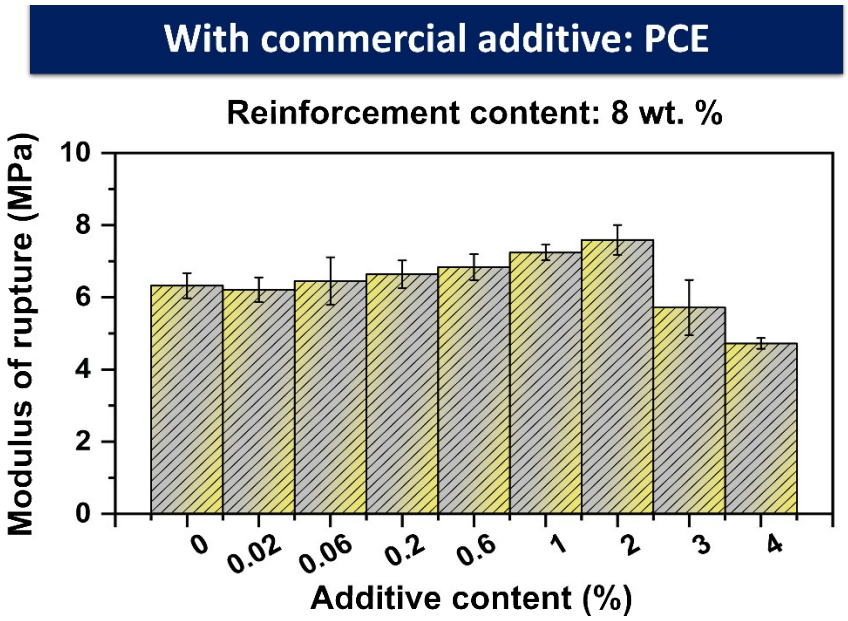

Figure S5. Mechanical characterization of fiber (NBSK) cement system with PCE (commercial superplasticizer). The values of the modulus of rupture (MOR) were collected from our previous research and figure was re-plotted using Origin (v2023) — this is not a digitized plot.[7] The commercial plasticizer was derived from petrochemical sources, and it belongs to the class polycarboxylate ether (PCE).

Rheological Characterization

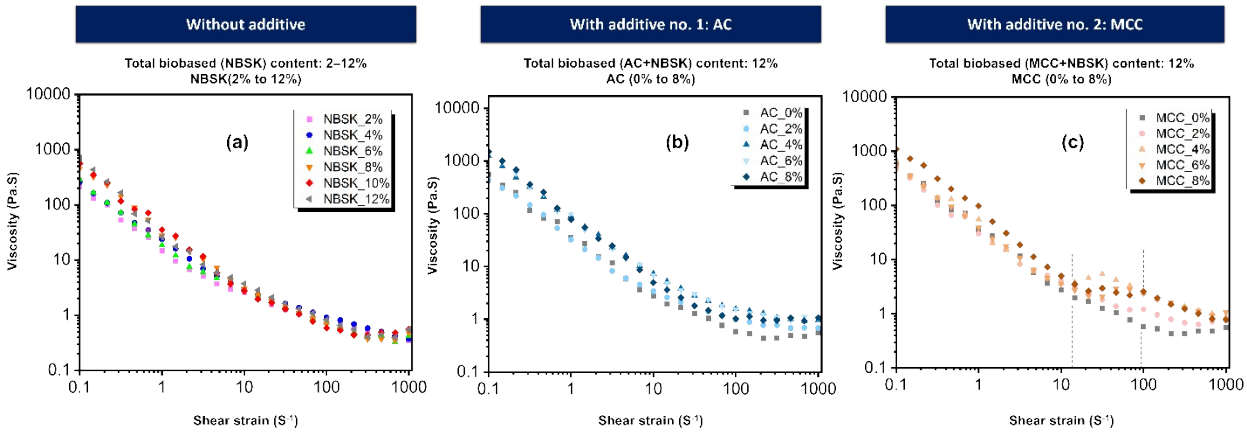

Figure S6. Steady-state viscometry of fiber cement slurry. The steady-state viscometry analysis of fiber cement samples containing varying proportions of reinforcing fibers and micro-cellulosic materials (a) NBSK fibers (b) NBSK and AC (c) NBSK and MCC, which are denoted as combination 1 and combination 2, respectively. Note that the dotted arrow tentatively depicts the boundaries of the constant viscosity region (observed with the addition of MCC in fiber cement slurry).

Figure S6 represents the evolution of shear viscosity by shear rate, under steady-state viscometry. As observed, in the case of all cement pastes, they follow a shear-thinning behavior.[7] Under high shear rates, the difference between shear viscosities of all formulations is minimal and they all reach a plateau. This is useful for applications where the slurry needs to be agitated at a high speed (e.g., >1000 rpm for pumping application of cement slurry) and an estimate of shear viscosity is required for determining the mixing requirements (factors such as binder ratio, water/cement ratio, content of fibers/additives).[13,14]

Under low shear rates, the shear viscosity of the fiber cement slurry increased as a function of the content of NBSK (from 2–12wt.%), AC, and MCC (from 2–8wt.%) as displayed in **Figure S6(a-c)** respectively. Such behavior was also observed with the addition of CNCs in fiber-cement slurry.[7] Note that, unlike NBSK fibers and AC, when MCC was added, the shear viscosity plot did not manifest a shear-thinning plot followed by the plateau in viscosity. Interestingly, the slurries follow a three-region shear-thinning flow, followed by a constant shear viscosity, which was previously reported for the case of biobased colloidal suspensions[15], emulsions[16], and slurries[17] (for e.g. CNC suspension/colloids in water).[18] Now, in some of these systems, aggregation of the agglomerates and their following de-aggregation under shear forces would introduce secondary shear-thinning behaviors in the viscosity plots.[17]

Hydration Products Characterization

The reaction of cement clinker phases (C_3S, C_2S, C_3A, C_4AF) with water results in an exothermic reaction, which results the formation of cement hydration products. For example, calcium silicate hydrate (CSH), portlandite ($Ca(OH)_2$), calcite ($CaCO_3$), ettringite ($C_6AS_3H_{32}$),

critical to strength development to the cement composite. The general cement hydration reaction is as follows:[19]

$$C_3S + 3CSH_2 + 26H \rightarrow C_6AS_3H_{32} \quad (2)$$

$$2C_3S + 6H \rightarrow C_3S_2H_3 + 3CH \quad (3)$$

$$2C_3A + 3C_6AS_3H_{32} + 22h \rightarrow 3C_4ASH_{18} \quad (4)$$

$$2C_2S + 4H \rightarrow C_3S_2H_3 + CH \quad (5)$$

$$C_4AF + 3CSH_2 + 3H \rightarrow C_6(AF)S_3H_{32} + (A,F)H_3 + CH \quad (6)$$

$$C_4AF + C_6(AF)S_3H_{32} + 2CH + 23H \rightarrow 3C_4(AF)SH_{18} + (A,F)H_3 \quad (7)$$

Where,
C_3S - Tricalcium silicate (Alite), C_2S - Dicalcium silicate(Belite), C_3A - Tricalcium aluminate, C_4AF - Tetracalcium aluminoferrite(Brown millerite),
$C_3S_2H_3$ - Gypsum

Cement hydration products were characterized through powder X-ray diffraction (PXRD) from Bruker, Germany (Model: D8 – advance). After curing for 28 days, a small portion of the composite was first mechanically disintegrated into powder using a tabletop grinder (Black+Decker, USA), and then sieved through a Canadian standard testing sieve (manufactured by W.S. Tyler, USA) with a mesh size (MS) of 100.

The diffraction experiment was performed in a typical Bragg-Brentano reflective geometry configuration [20] with parameters akin to those of our earlier report.[7]

(a)

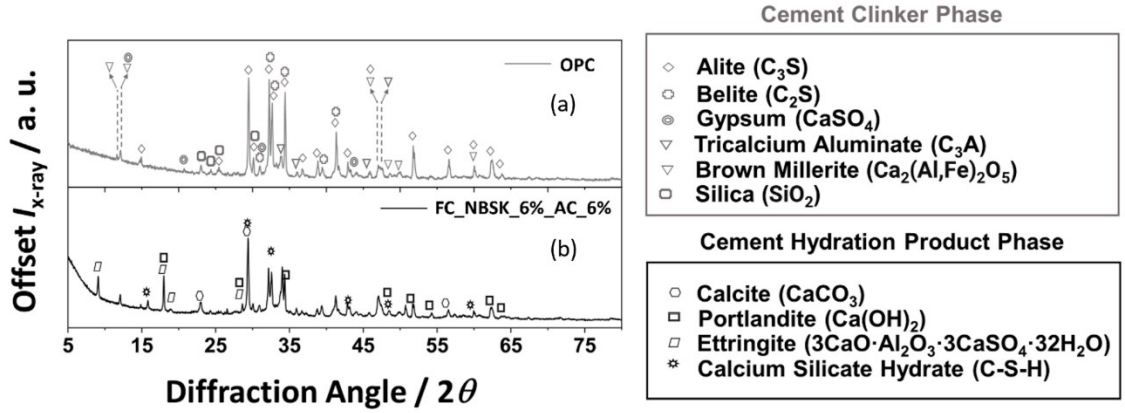

(c)

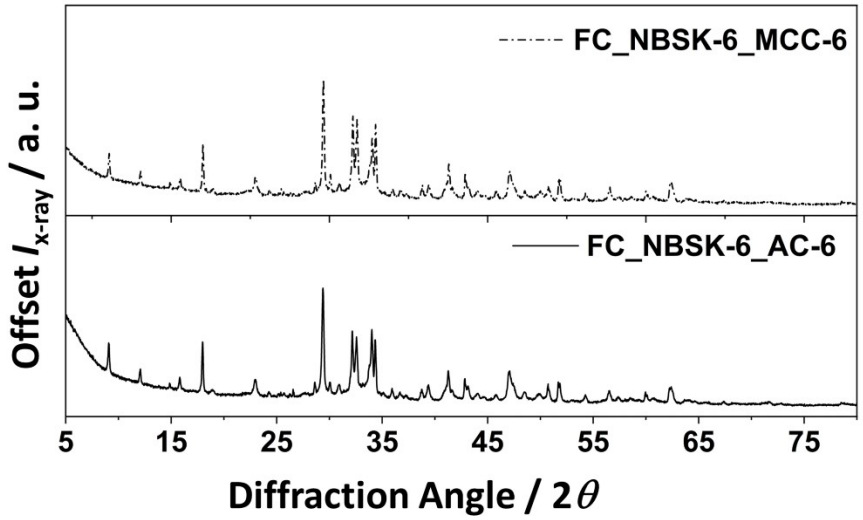

Figure S7 Hydration products characterization. Powder X- Ray diffractogram (PXRD) of (a) OPC clinker phases (b) and (c) representative fiber cement sample containing both combinations, depicting their OPC hydration products.The powder diffraction file (PDF) number associated with the OPC clinker phases and fiber cement hydration products (as obtained from ICSD database) is as follows: Alite (00-055-0738), Belite (00-033-0302), Gypsum (01-074-1905), Tricalcium aluminate (01-074-7039), Brownmillerite (01-074-3674), Silica (01-071-0261), calcite (01-086-2334), portlandite (00-001-1079), Ettringite (01-075-7554).

From **Figure S7**, strong reflection peaks were observed at 8° and 17°, corresponding to ettringite and portlandite phases, which were absent in the PXRD diffractogram of anhydrate OPC samples, thereby conforming the presence of cement hydration products. Irrespective of the micro-cellulosic materials, the phase identification revealed the presence of typical cement hydration products like portlandite, ettringite, and calcite (*vide supra*). In addition to these, peak overlaps between calcium silicate hydrate (CSH) and ettringite phases cause difficulties in decoupling the interference between these phases and identifying them unambiguously. To ascertain this, we followed the recent work conducted by Maddalena et al., and we tentatively assigned the reflection peak at 16°, 29°, 32° and 49° for CSH. [21] There is also peak overlapping observed between calcite and CSH peaks at 29°, the reason being that, even though we covered our samples using a plastic

bag during curing, there could be some interference of air, reaction between CO_2 with the calcium hydroxide to form calcium carbonate is possible.[22]

Cost/Performance Analysis

Table S11. The table depicting the material cost (reinforcement/additive) for fabricating all the FC samples used in this research.

Sample ID	NBSK fibers (wt.% of cement)	w/c ratio	Additive (wt.% of cement)		Cost of reinforcement (USD/g)	Cost of additive (USD/g)	Total Cost (USD)
Without additive							
			AC	**MCC**			
NBSK_2%	2 (8.4 g)	0.5	-	-	0.003	-	0.02
NBSK_4%	4 (16.8 g)	0.5	-	-	0.003	-	0.05
NBSK_6%	6 (25.2 g)	0.5	-	-	0.003	-	0.07
NBSK_8%	8 (33.6 g)	0.5	-	-	0.003	-	0.1
NBSK_10%	10 (42 g)	0.5	-	-	0.003	-	0.12
NBSK_12% (Control sample)	12 (50.4 g)	0.5	-	-	0.003		0.15
NBSK 16%	16 (67.2 g)	0.5	-	-	0.003	-	0.2016
NBSK 24%	24 (100.8 g)	0.5	-	-	0.003	-	0.3024
NBSK 32%	32 (134.4 g)	0.5	-	-	0.003	-	0.4032
Combination 1: AC and NBSK							
			AC	**MCC**			
AC_2%	10 (50.4 g)	0.5	2 (8.4 g)	-	0.003	0.0008	0.126
AC_4%	8 (33.6 g)	0.5	4 (16.8 g)	-	0.003	0.0008	0.113
AC_6%	6 (25.2 g)	0.5	6 (25.2 g)	-	0.003	0.0008	0.09
AC_8%	4 (16.8 g)	0.5	8 (33.6 g)	-	0.003	0.0008	0.07
AC_10%	2 (8.4 g)	0.5	10 (42 g)	-	0.003	0.0008	0.0588
Combination 2: MCC and NBSK							
				AC	**MCC**		
MCC_2%	10 (50.4 g)	0.5	-	2 (8.4 g)	0.003	0.0045	0.16
MCC_4%	8 (33.6 g)	0.5	-	4 (16.8 g)	0.003	0.0045	0.17
MCC_6%	6 (25.2 g)	0.5	-	6 (25.2 g)	0.003	0.0045	0.18
MCC_8%	4 (16.8 g)	0.5	-	8 (33.6 g)	0.003	0.0045	0.20
Combination 3: CNC and NBSK (previous study)[7]							
Sample ID	**NBSK fibers (wt.% of cement)**	**w/c ratio**	**Additive (wt.% of cement)**	**Cost of reinforcement (USD/g)**	**Cost of additive (CNC) (USD/g)**	**Total Cost (USD)**	
CNC_2%	8 (33.6 g)	0.5	2 (8.4 g)	0.003	0.007	0.1588	
CNC_4%	8 (33.6 g)	0.5	4 (16.8 g)	0.003	0.007	0.2176	

The cost of NBSK fibers is inclusive of the refining cost mentioned in **Table S12**. Note that the total cost here refers to the total (reinforcement + additive) cost that is required to produce a fiber cement composite as mentioned in the manuscript. The raw material cost is derived from **Table S12** (*vide infra*) to tabulate the total reinforcement cost. In **Table S11**, FC: Fiber cement, NBSK: Northern bleached softwood kraft pulp, AC: Alpha cellulose, MCC: Microcrystalline cellulose.

Table S12. Table representing the reinforcement/additive cost (adapted from current market prices and prior in depth technoeconomic studies conducted to ascertain the production cost of these additives) along with their references.

Materials	Cost (USD / Mt)		Reference
Cellulosic fiber			
NBSK	Raw material	≈ 700	[24,25]
	Refining	≈ 1720	
	Total	≈ 2420	
Cellulosic additive			
AC	≈ 800		[26,27]
MCC	≈ 4500		[28,29]
CNC	≈ 7000		[27,30]

As shown in **Figure S12**, the total production cost of NBSK fibers (raw material cost + cost of refining) makes them an expensive component in the fiber cement, where the cost of production of cement is around only 60 USD/tonne).[31] Additionally fiber refining is an energy-intensive process and modeling studies from Chakraborty et al., reveals that the cost of refining 1 kg of NBSK fibers (to 1 μm length) in a PFI mill was accounted to about USD 1.72/kg (ca. two times the cost to procure 1 tonne of NBSK fibers).[25]

High content of NBSK fibers demands the use of additional rheology modifiers/superplasticizer, which is another significant contributor to carbon dioxide emissions as well as added cost to a fiber cement fabrication process. For example, the cost of production of PCE superplasticizer is about 850–1440 USD/tonne).[32] Thus, "*less is more*" is the philosophy followed in this research work so that we do not have to compromise with performance metrics without incorporating property-specific additives like curing accelerators, and retarders, to name a few.

Table S13. Cost of silica-based additives used in construction industry. Note that these prices can fluctuate depending on market trends and product availability.

	Cost USD/mt	**Reference**
Silica fume (Micro silica)	200 - 800	[33]
Silica sand	90	[34]
Nano silica	1500 – 4000 *Could be even higher depending upon the size and purity	[35]

As seen from **Table S13,** the cost of silica-based additives varies with the size and type of silica, most common are silica sand (low-cost) and micro silica. Though silica sand is cheap, extracting sand would involve quarrying activities to be conducted, causing significant environmental impact. In terms of micro silica, the prices can be compared with that of AC, indicating the cost feasibility in replacing silica-based additives with bio-based (cellulosic) additives for building materials.

References

1 N. B. Singh, *Smart Nanoconcretes and Cement-Based Materials: Properties, Modelling and Applications*, 2020, 9–39.

2 Portland Cement | Lafarge Canada, https://www.lafarge.ca/en/portland-cement, (accessed 1 January 2024).

3 Avicel® PH-101 - Cellulose, Cellulose powder, https://www.sigmaaldrich.com/CA/en/substance/avicelph101123459004346, (accessed 2 August 2023).

4 Nanocellulose Data Sheets - The Process Development Center - University of Maine, https://umaine.edu/pdc/nanocellulose/nanocellulose-spec-sheets-and-safety-data-sheets/, (accessed 4 August 2022).

5 Bleached Softwood Kraft Pulp | Canfor, https://www.canfor.com/products/pulp-and-paper/pulp/bleached-softwood-pulp, (accessed 4 August 2022).

6 Pulp bleaching sequences | pulp paper mill, https://www.pulppapermill.com/pulp-bleaching-sequences/, (accessed 1 January 2024).

7 S. Raghunath, M. Hoque and E. J. Foster, *ACS Sustain Chem Eng*, DOI:10.1021/acssuschemeng.3c01392.

8 L. Segal, J. J. Creely, A. E. Martin and C. M. Conrad, *Textile Research Journal*, 1959, **29**, 786–794.

9 A. Khenblouche, D. Bechki, M. Gouamid, K. Charradi, L. Segni, M. Hadjadj and S. Boughali, *Polímeros*, 2019, **29**, e2019011.

10 O. A. Adeleye, O. A. Bamiro, D. A. Albalawi, A. S. Alotaibi, H. Iqbal, S. Sanyaolu, M. N. Femi-Oyewo, K. O. Sodeinde, Z. S. Yahaya, G. Thiripuranathar and F. Menaa, *Materials*, DOI:10.3390/MA15175992.

11 S. Park, J. O. Baker, M. E. Himmel, P. A. Parilla and D. K. Johnson, *Biotechnol Biofuels*, 2010, **3**, 1–10.

12 Cellulose nanowhiskers isolation and properties from acid hydrolysis combined with high pressure homogenization: BioResources, https://bioresources.cnr.ncsu.edu/resources/cellulose-nanowhiskers-isolation-and-properties-from-acid-hydrolysis-combined-with-high-pressure-homogenization/, (accessed 25 August 2024).

13 D. Han and R. D. Ferron, *Constr Build Mater*, 2015, **93**, 278–288.

14 W. Piasta and B. Zarzycki, *Constr Build Mater*, 2017, **140**, 395–402.

15 F. Pignon, M. Challamel, A. De Geyer, M. Elchamaa, E. F. Semeraro, N. Hengl, B. Jean, J. L. Putaux, E. Gicquel, J. Bras, S. Prevost, M. Sztucki, T. Narayanan and H. Djeridi, *Carbohydr Polym*, 2021, **260**, 117751.

16 K. F. Wissbrun, *J Rheol (N Y N Y)*, 1981, **25**, 619–662.

17 A. Ahuja, A. Potanin and Y. M. Joshi, *Adv Colloid Interface Sci*, 2020, **282**, 102179.

18 B. Zakani, H. Salem, S. Entezami, A. Sedaghat and D. Grecov, *Cellulose*, 2022, **29**, 3963–3984.

19 Hydration, https://www.engr.psu.edu/ce/courses/ce584/concrete/library/construction/curing/Hydration.htm, (accessed 5 March 2023).

20 M. Deutsch, G. Hölzer, J. Härtwig, J. Wolf, M. Fritsch and E. Förster, *Phys Rev A*, 1995, **51**, 283–296.

21 R. Maddalena, K. Li, P. A. Chater, S. Michalik and A. Hamilton, *Constr Build Mater*, 2019, **223**, 554–565.

22 D. Xie, S. Yao, J. Cao, W. Hu and Y. Qin, *Mar Pet Geol*, 2020, **117**, 104376.

23 G. Robertson, J. Olson, P. Allen, B. Chan and R. Seth, Measurement of fiber length, coarseness, and shape with the fiber quality analyzer, TAPPI JOURNAL, O, https://imisrise.tappi.org/TAPPI/Products/99/OCT/99OCT93.aspx, (accessed 24 November 2023).

24 Canfor, *CANFOR PULP REPORTS RESULTS FOR SECOND QUARTER OF 2023*, 2023.

25 A. Chakraborty, M. M. Sain, M. T. Kortschot and S. B. Ghosh, Modeling energy consumption for the generation of microfibres from bleached kraft pulp fibres in a PFI mill: BioResources, https://bioresources.cnr.ncsu.edu/resources/modeling-energy-consumption-for-the-generation-of-microfibres-from-bleached-kraft-pulp-fibres-in-a-pfi-mill/, (accessed 27 November 2023).

26 Alpha Cellulose (Cotton), https://www.indiamart.com/proddetail/alpha-cellulose-fiber-2852563247262.html, (accessed 1 January 2024).

27 C. Abbati De Assis, C. Houtman, R. Phillips, T. Bilek, O. J. Rojas, M. S. Peresin, H. Jameel and R. Gonzalez, DOI:10.1002/bbb.1782.

28 R. Sri Bhanupratap Rathod, P. Sahoo and S. Gupta, *Constr Build Mater*, 2023, **385**, 131531.

29 K. M., Vanhatalo, K. E., Parviainen and O. P. Dahl, Techno-economic analysis of simplified microcrystalline cellulose process :: BioResources, https://bioresources.cnr.ncsu.edu/resources/techno-economic-analysis-of-simplified-microcrystalline-cellulose-process/, (accessed 1 January 2024).

30 R. Ciriminna, M. Ghahremani, B. Karimi and M. Pagliaro, *Biofuels, Bioproducts and Biorefining*, 2023, **17**, 10–17.

31 O. Oguntola and S. Simske, *Resources 2023, Vol. 12, Page 95*, 2023, **12**, 95.

32 PCE, (2024), https://www.zauba.com/import-polycarboxylate-ether-cement-hs-code.html, (accessed 1 January 2024).

33 Silica fume price per kg - HSA Microsilica, https://microsilica-fume.com/silica-fume-price-per-kg.html, (accessed 2 June 2024).

34 Silica Sand Price in Canada - 2023 - Charts and Tables - IndexBox, https://www.indexbox.io/search/silica-sand-price-canada/, (accessed 2 June 2024).

35 Nano Silica Price, 2024 Nano Silica Price Manufacturers & Suppliers | Made-in-China.com, https://www.made-in-china.com/products-search/hot-china-products/Nano_Silica_Price.html, (accessed 2 June 2024).